

MINIMIZATION OF VIBRATION IN AERONAUTICAL WING SPARS UNDER FLUTTER SITUATION

LARISSA SANTOS¹, MARCELO ARAUJO SILVA² AND REYOLANDO BRASIL³

¹Federal University of ABC
Av. dos Estados, 5001, Bangu, Santo André - SP, Brazil, Postal Code: 09210-580
larissa.teixeira@aluno.ufabc.edu.br

²Affiliation
Postal Address
E-mail address and URL

³ Affiliation
Postal Address
E-mail address and URL

Key words: Vibrations, Flutter, Aeroelasticity, Structure, Aeronautical Wings.

Abstract. This research project aims to investigate the mitigation of vibrations in the spars of aeronautical wings during flutter occurrences. The study will delve into aeroelastic phenomena, particularly focusing on flutter, defined as the self-excited interaction of vibration modes within a modified system, which can potentially lead to catastrophic failures. An analytical method has been developed to compute the flutter velocity, considering the stiffness and mass matrices, and the utilization of a Tuned Mass Damper (TMD) has been proposed to enhance the flutter velocity, thereby extending the aircraft's operational range. Suggestions for future research directions have been provided.

1 INTRODUCTION

In the present study, we will investigate the flutter phenomenon in an aeronautical wing. The typical translation of the word "flutter" from English to Portuguese is "draping," describing the motion that flags exhibit when stirred by the wind. Similarly, this phenomenon occurs in aeronautical wing structures when the relative air displacement reaches a critical velocity threshold. To mitigate this effect and enhance the relative displacement speed of an aircraft, we will design a Tuned Mass Damper (TMD). As demonstrated later, this device can expand the range of velocities before flutter occurs. Subsequently, we will outline the three primary topics encompassed in this investigation.

2 VIBRATIONS

Dynamics, rooted in Newton's laws, pertains to the interaction of forces applied to bodies, leading to displacements. Structures, being bodies, respond to forces by generating inertial forces. Structural analysis adheres to the scientific method: observation, hypothesis formulation, testing, analysis of results, test repetition, and conclusion. Testing involves

constructing a mathematical model with solutions grounded in the laws of mechanics. A one-degree-of-freedom model characterizes systems controlled by a single coordinate. Common models encompass undamped free vibrations and damped vibrations, with equations of motion derived from Newton's second law. These equations can be solved either analytically or numerically.

2.1 Damped Free Vibrations

The mathematical model of the spring-mass system depicted in Figure 1 adheres to the principles of mechanics. Upon application of a horizontal force $P(t)$ to the mass, the spring reacts with an elastic restoring force proportional to the displacement (u) and a damping force proportional to the velocity \dot{u} .

Like, this,

$$f_i = P(t) - f_e - f_d, \quad (1)$$

which, rearranged, falls into the well-known form of the Equation of Motion of a one-degree-of-freedom system, the ordinary differential equation (ODE):

$$M\ddot{u} + C\dot{u} + Ku = P(t) \quad (2)$$

A case of interest is when the system is free, that is, without the external force $P(t)$, and without damping, where the equation falls back on that shown in Eq. (3). In this case, the only possible movements are due to the initial displacement conditions, u_0 , and speed, \dot{u}_0 . The EDO becomes.

$$M\ddot{u} + Ku = 0, \quad (3)$$

Where

$$\omega = \sqrt{\frac{K}{M}} \quad (4)$$

is the undamped circular frequency of the system (in rad/s, in SI). The cyclic frequency (in Hz, or cycles per second) is

$$f = \frac{\omega}{2\pi}, \quad (5)$$

whose inverse is the period of free vibration (in seconds),

$$T = \frac{1}{f} = \frac{2\pi}{\omega}. \quad (6)$$

What is being said is that when the structure is put in motion, it will vibrate harmonically

with frequency, that is, it will repeat the movement that number of times in each second. The period is the time interval between the peaks of this movement. Both frequency and period are properties of the structure and are called “natural”.

This harmonic response, dependent on the initial conditions, can be written as

$$u(t) = \rho \cos(\omega t + \theta) \quad (7)$$

Considering the presence of damping, as is necessary in real structures, we have the ODE

$$M\ddot{u} + C\dot{u} + Ku = 0, \quad (8)$$

Or

$$\ddot{u} + 2\xi\omega\dot{u} + \omega^2 u = 0, \quad (9)$$

The solution to the ordinary differential equation (ODE) is:

$$u(t) = e^{-\xi\omega t} \rho \cos(\omega_D t + \theta), \quad (10)$$

Note that the resultant harmonic motion (Figure 1) experiences a rapid decline in amplitude owing to the negative exponential term it multiplies, while its frequency is slightly diminished by damping. Consequently, the corresponding period is slightly extended.

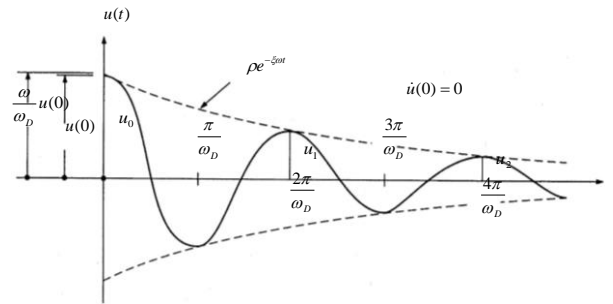


Figure 1 - Response to free vibration of a system with subcritical damping

In the context of flutter, which is the central focus of this study, it essentially represents a damped free system. However, an instability phenomenon arises wherein, contrary to the diminishing displacements observed in Figure 4, there is a progressive increase in displacement. This escalation in displacement can potentially lead to the system's failure.

3 FLUTTER

Flutter is a self-excited vibration in which an elastic body immersed in a flow gains energy from the fluid, resulting in continuous oscillations determined by the body itself. It's a natural response, unlike forced vibrations like resonance. Aircraft structures, due to their flexibility, experience various distortions under load, known as aerelasticity, leading to problems like flutter, buffeting, and dynamic response. Flutter, the most studied aerelastic phenomenon, occurs when two or more vibration modes couple, leading to unstable oscillations. The critical flutter velocity is reached when damping becomes zero. Cantilevered aircraft wings experience

flutter due to coupling of torsional and translational degrees of freedom. Solving flutter problems can be done in time or frequency domains, with frequency domain methods being computationally efficient.

3.1 The Flutter Equations

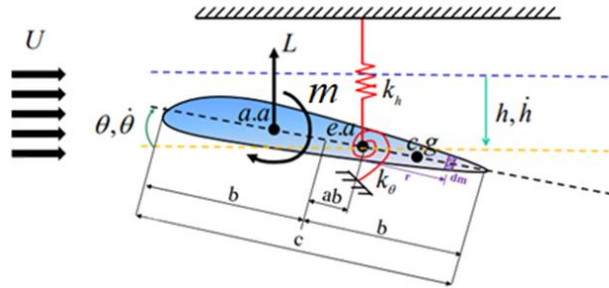


Figure 2 - Representation of the variables involved

Using the equations of Lagrangian mechanics, in the model shown in Figure 2, one can develop the free vibration equation, with two degrees of freedom, given by (Cardoso, 2022).

$$\begin{bmatrix} M & -Mb(a - e) \\ -Mb(a - e) & I_p \end{bmatrix} \begin{bmatrix} \ddot{h} \\ \ddot{\theta} \end{bmatrix} + \begin{bmatrix} k_h & qSC_{L\theta} \\ 0 & k_\theta \end{bmatrix} \begin{bmatrix} h \\ \theta \end{bmatrix} = \begin{bmatrix} 0 \\ 0 \end{bmatrix}, \quad (11)$$

is the dynamic air pressure, ρ is the air density, S is the area of the airfoil section, and a is a dimensionless variable that describes the position of the center of gravity as a function of b and CL_q is the slope of the lift coefficient curve as a function of the angle of attack q .

Equation (11) can be rewritten matrixly as

$$M\ddot{u} + Ku = 0 \quad (12)$$

Where, M is the mass matrix, K the stiffness matrix, \ddot{u} the acceleration vector and u the displacement vector.

To determine the natural frequencies of vibration of the system, the following eigenvalue problem is solved:

$$\det(K - p^2M) = 0 \quad (13)$$

When it reaches a so-called critical value, instability occurs. The solution to equation (13) is given by:

$$p_j = d_j + \omega_j i \quad (14)$$

where d_j is the real component and ω_j the imaginary component of the complex roots.

$$u(t) = e^{d_j t} (\cos \omega_j t + i \operatorname{sen} \omega_j t) \quad (15)$$

The imaginary component ω_j of Equation 14 generates a harmonic oscillator in Equation 15. When d_j is zero, simple harmonic motion occurs. But when d_j becomes non-zero, flutter can occur. If d_j is negative, damped free vibration occurs.

4 TUNED MASS DAMPER

A Tuned Mass Damper (TMD) is a system engineered to diminish vibration amplitudes by absorbing kinetic energy. It comprises a mass-spring system adjusted to the primary structure to attenuate oscillations. Integration of a TMD alters the system's frequencies, thus enhancing dynamic performance and preventing resonance. In flutter scenarios, the objective is to maximize the critical speed, enabling higher-speed operations with reduced displacements. Design parameters for TMD entail the natural frequency ratio between TMD and primary structure, as well as the mass ratio. The TMD dissipates energy through vibration, thereby decreasing the amplitude of structural motions. This study focuses on employing a TMD to alleviate flutter-induced vibrations in an aircraft wing spar, thereby broadening the operational speed range of the aircraft.

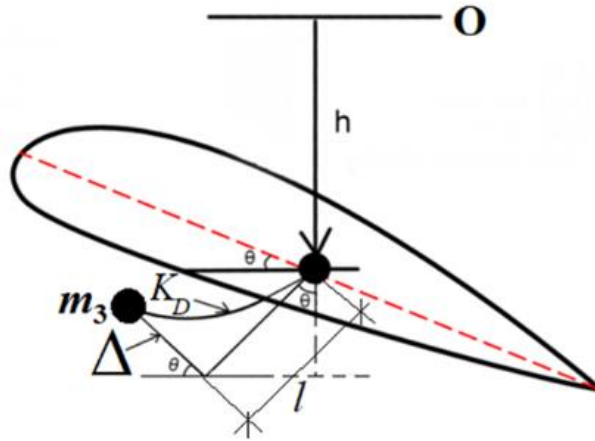


Figure 3 - Model including the TMD

To develop the TMD matrices, being the stiffness and mass matrices, one must first find the values of the stiffness of the TMD rod (K_D) and the equivalent mass at its end.

$$K_D = 3 \frac{EI_\Delta}{l^3} \quad (16)$$

The mass of the TMD (M_D):

$$M_D = \frac{\rho_\Delta l}{4} + m_3 \quad (17)$$

The kinetic energy (T) of the TMD is given by:

$$T = \frac{1}{2} M_D (\dot{v}^2 + \dot{u}^2) \quad (18)$$

Thus, using the equations of Lagrangian mechanics, one can find the TMD mass matrices (MD).

$$\mathbf{M}_{\Delta} = \begin{bmatrix} M_{\Delta} & 0 & 0 \\ 0 & M_{\Delta}l^2 & M_{\Delta}l \\ 0 & M_{\Delta}l & M_{\Delta} \end{bmatrix} \quad (19)$$

And using Hooke's Law, the TMD stiffness matrix is determined to be

$$\mathbf{K}_{\Delta} = \begin{bmatrix} 0 & 0 & 0 \\ 0 & 0 & 0 \\ 0 & 0 & K_{\Delta} \end{bmatrix}. \quad (20)$$

Adding these matrices with those already obtained for flutter, we have

$$\mathbf{M} = \begin{bmatrix} M + M_{\Delta} & -Mb(a - e) & 0 \\ -Mb(a - e) & I_p + M_{\Delta}l^2 & M_{\Delta}l \\ 0 & M_{\Delta}l & M_{\Delta} \end{bmatrix} \quad (21)$$

And

$$\mathbf{K} = \begin{bmatrix} k_h & qSC_{L\theta} & 0 \\ 0 & k_{\theta} & 0 \\ 0 & 0 & K_{\Delta} \end{bmatrix}. \quad (22)$$

With the matrices M and K described above, the optimization of the TMD design is undertaken, the formulation of which will be presented in the subsequent section.

5 OPTIMIZED TMD DESIGN

For the TMD project, an optimization problem was defined, as follows. Determine $\mathbf{x} \in \mathbb{R}^3$, onde $\mathbf{x} = [x_1 \ x_2 \ x_3]^T = [U \ h_D \ M_D]^T$, that minimizes the function $f(\mathbf{x}) = -x_1$,

Subject to

$$\begin{aligned} g_1 &= -|l_1 - l_2| + e \leq 0 \\ g_2 &= -|l_2 - l_3| + e \leq 0 \\ g_3 &= -|l_1 - l_3| + e \leq 0 \\ g_4 &= -D_b + e \leq 0 \\ g_5 &= m_D - m_{lim} \leq 0 \end{aligned}$$

where h_D is the height of the cross-section of the TMD, l_i , $i = 1,2,3$ are the problem eigenvalues of $|\mathbf{K} - \lambda\mathbf{M}| = 0$, e is a small number (equal to 0.1) to force convergence, D_b is the radicand of Bhaskara's formula for calculating l_2 and l_3 , m_D is the ratio between the mass of the TMD and the mass of the main structure and m_{lim} is the threshold value of m_D , equal to

0.05. The optimization problem then consists of maximizing the value of the critical flutter velocity.

6 RESULTS OBTAINED

This chapter presents the results obtained from the conducted studies, employing an aeroelastic model of an airfoil. In this model, the spar comprises a rectangular section fabricated from a composite material, while the TMD is constructed from aeronautical aluminum. The adopted data include:

$$a = -0.15.$$

$$b = 0,127 \text{ m};$$

$$e = 0,25;$$

$$M = 4,7174 \text{ kg};$$

$$I_p = 1,543 \text{ kg.m}^2;$$

$$k_h = 16282 \text{ N/m};$$

$$k_q = 5816 \text{ N.m/rad};$$

$$K_{12} = 2,93 \text{ U}^2;$$

$$ED = 70 \text{ GPa}; \text{ (modulus of elasticity of the TMD material)}$$

$$r_D = 2600 \text{ kg/m}^3; \text{ (TMD material density)}$$

$$b_D = 30 \text{ mm}; \text{ (base of the TMD cross section)}$$

$$l = 130 \text{ mm}. \text{ (TMD rod length)}$$

The ultimate design of the TMD, employing the GRG (Generalized Reduced Gradient) method, yielded $x = [21.63 \text{ m/s } 0.178 \text{ mm } 0.236 \text{ kg}]^T$. Consequently, by computing the eigenvalues of the problem $|K - \lambda M| = 0$ and determining the natural frequencies of vibration, the graphs depicted in Figures 4 and 5 were generated.

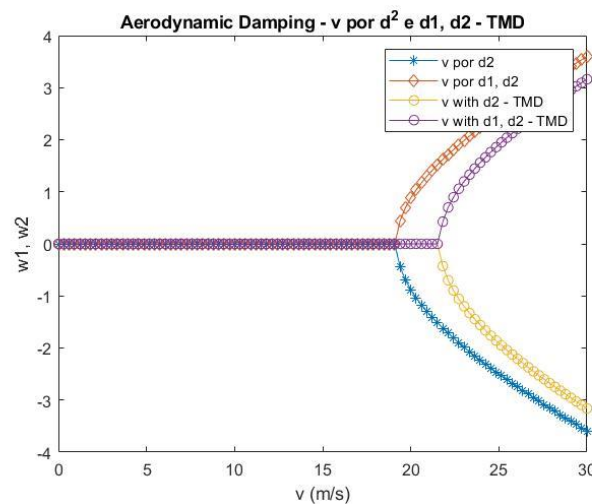


Figure 4 - Graph of aerodynamic damping with and without TMD

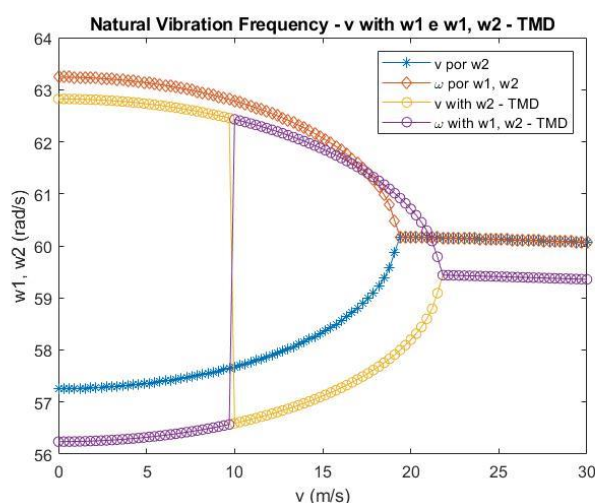


Figure 5 - Graph of the natural frequency of vibration without TMD

It can be seen in Figures 8 and 9 that TMD increased the critical flutter velocity from 19.18 m/s (without TMD) to 21.63 m/s, that is, a 13% increase in the range of possible flutter velocity aircraft operation. The result shows that the TMD can be very useful for the design of aircraft spars.

7 CONCLUSIONS

The flutter phenomenon was mathematically modeled following the theory proposed by Cardoso (2022). Stiffness and mass matrices were constructed for a two-degree-of-freedom model, with the introduction of a third degree of freedom associated with the TMD. In this study, the TMD was depicted as a flexible rod integrated into the primary structure.

Two scenarios were examined to illustrate the structural behavior under flutter conditions: one without the TMD and the other with the TMD installed. The results demonstrated a 13% increase in the aircraft's operational speed range with the implementation of the TMD.

Consequently, it was concluded that employing TMD can significantly enhance the design of aircraft spars by extending the operational range. For future research endeavors, it is recommended to explore different types of TMDs using time domain analysis, imposing constraints on dynamic displacements, and setting a lifespan for the structure, even during an instability process.

REFERENCES

- [1] Jianhong, W. e Ramirez-Mendoza, RA (2023), "Estratégia direta baseada em dados para teste de vibração de aeronaves em circuito fechado", *Engenharia de Aeronaves e Tecnologia Aeroespacial*, Vol. 95 No. 5, pp. <https://doi.org/10.1108/AEAT-09-2022-0264>. Acesso em: 29/08/2023.
- [2] Wang, X. , Liu, Z. , Guo, L. , Lv, J. e Ji, C. (2022), "Simulações aeroelásticas no domínio do tempo baseadas em CFD de uma aeronave de fuselagem dupla", *Engenharia de Aeronaves e Tecnologia Aeroespacial*, vol. 94 No. 10, pp. [8](https://doi.org/10.1108/AEAT-

</div>
<div data-bbox=)

- 08-2021-0261. Acesso em: 29/08/2023.
- [3] Rogólski, R. e Olejnik, A. (2018), "Modelo estrutural com controles de um avião muito leve para cálculos numéricos de vibração", *Engenharia de Aeronaves e Tecnologia Aeroespacial*, Vol. 92 N° 3, pp. <https://doi.org/10.1108/AEAT-01-2018-0059>. Acesso em: 29/08/2023.
- [4] Jianhong, W. (2021), "Projeto de sinal de entrada ideal para identificação de parâmetros de modelo de vibração de aeronaves", *Engenharia de Aeronaves e Tecnologia Aeroespacial*, Vol. 93 N° 10, pp. <https://doi.org/10.1108/AEAT-09-2020-0205>. Acesso em: 29/08/2023.
- [5] Azadi, M. (2018), "Supressão de vibração de um feixe FGM termoelástico sujeito à força do seguidor", *Engenharia de Aeronaves e Tecnologia Aeroespacial*, Vol. 90 No. 9, pp. <https://doi.org/10.1108/AEAT-05-2016-0089>. Acesso em: 29/08/2023.
- [6] Chajec, W. (2018), "Comparação de métodos de cálculo de vibração com base no resultado do teste de vibração do solo", *Engenharia de Aeronaves e Tecnologia Aeroespacial*, Vol. 91 No. 3, pp. <https://doi.org/10.1108/AEAT-03-2018-0102>. Acesso em: 29/08/2023.
- [7] Bruni, C., Cestino, E. e Frulla, G. (2016), "Análise paramétrica de uma asa piezoelétrica vibrante", *Engenharia de Aeronaves e Tecnologia Aeroespacial*, Vol. 88 N° 3, páginas 382-388. <https://doi.org/10.1108/AEAT-02-2014-0024>. Acesso em: 29/08/2023.
- [8] F., PC, Samikkannu, R., Sura, NK e Mulla, S. (2018), "Modelagem aeroelástica baseada em identificação de sistema para vibração de asa", *Engenharia de Aeronaves e Tecnologia Aeroespacial*, Vol. 90 No. 2, pp. <https://doi.org/10.1108/AEAT-08-2016-0122>. Acesso em: 29/08/2023.
- [9] Fatehi, M., Moghaddam, M. e Rahim, M. (2012), "Análise robusta de vibração e controle de uma asa", *Engenharia de Aeronaves e Tecnologia Aeroespacial*, Vol. 84 N° 6, pp. <https://doi.org/10.1108/00022661211272981>. Acesso em: 29/08/2023.
- [10] Pankaj, AC, Shanthini, G., Shivaprasad, MV e Manjuprasad, M. (2013), "Predição de vibração de aeronaves usando parâmetros modais experimentais", *Engenharia de Aeronaves e Tecnologia Aeroespacial*, Vol. 85 N° 2, pp. <https://doi.org/10.1108/00022661311302698>. Acesso em: 29/08/2023.~
- [11] Kayran, A. (2007), "Teste de vibração de voo e estabilidade aeroelástica de aeronaves", *Engenharia de Aeronaves e Tecnologia Aeroespacial*, Vol. 79 N° 2, pp. <https://doi.org/10.1108/00022660710732707>. Acesso em: 29/08/2023.
- [12] Ozdemir Ozgumus, O. e Kaya, MO (2007), "Formulação para análise de vibração e vibração de uma pá de helicóptero sem dobradiças pairando: parte II. Resultados da estabilidade de vibração e análise de vibração de uma pá de helicóptero sem dobradiças pairando", *Engenharia de Aeronaves e Tecnologia Aeroespacial*, Vol. 79 N° 3, pp. <https://doi.org/10.1108/00022660710743822>. Acesso em: 29/08/2023.
- [13] TANG, Haojun; LI, Yongle; MO, Wei. Aplicação de cabos cruzados para a estabilidade de vibração de uma ponte pênsil de longo vão durante a montagem. *Estruturas de Engenharia*, v. 276, 2023, p. 115354. ISSN0141-0296. Disponível em: <https://doi.org/10.1016/j.engstruct.2022.115354>. Acesso em: 29/08/2023.
- [14] Pradhan, S. e Datta, PK (2006), "Características de instabilidade dinâmica de uma estrutura de míssil livre sob uma força seguidora controlada", *Aircraft Engineering and Aerospace Technology*, Vol. 78 N° 6, pp. <https://doi.org/10.1108/00022660610707184>. Acesso em: 29/08/2023.
- [15] LIN, RM; NG, T.-Y. Identificação de kernels de Volterra para melhores previsões de

- respostas de vibração aeroelástica não linear e flutter. *Estruturas de Engenharia*, v. 171, 2018, p. 15-28. ISSN0141-0296. Disponível em: <https://doi.org/10.1016/j.engstruct.2018.05.073> . Acesso em: 29/08/2023.
- [16] WU, Lianhuo et al. Análise da diferença de fase de vibração em pontes suspensas de longo vão durante flutter. *Estruturas de Engenharia*, v. 276, 2023, p. 115351. ISSN0141-0296. Disponível em: <https://doi.org/10.1016/j.engstruct.2022.115351> . Acesso em: 29/08/2023.
- [17] MICHLER, C.; VAN BRUMMELEN, H.; DE BORST, R. Uma investigação de Interface-GMRES (R) para problemas de interação fluido-estrutura com vibração e divergência. *Comput Mech*, v. 47, p. 17-29, 2011. Disponível em: <https://doi.org/10.1007/s00466-010-0519-8>. Acesso em: 29/08/2023.
- [18] HELGEDAGSRUD, T. A. et al. Investigação computacional e experimental de vibração livre e flutter de tabuleiros de pontes. *Comput Mech*, v. 63, p. 121-136, 2019. Disponível em: <https://doi.org/10.1007/s00466-018-1587-4>. Acesso em: 29/08/2023.
- [19] MANAN, A. et al. Otimização de estruturas compostas aeroelásticas usando algoritmos evolutivos. *Otimização de Engenharia*, v. 42, n. 2, pág. 171-184, 2010. DOI: 10.1080/03052150903104358. Acesso em: 29/08/2023.
- [20] WOFF, JM; FLEETER, S. Aerodinâmica e vibração em cascata em oscilante viscosa por um método analítico local. *Mecânica Computacional*, v. 203-215, 1992. Disponível em: <https://doi.org/10.1007/BF00370089> . Acesso em: 29/08/2023.
- [21] ZHANG, LW; CANÇÃO, ZG; LIEW, KM Modelagem de propriedades aerotermoelásticas e controle ativo de flutter de cascas cilíndricas nanocompostas em fluxo de ar supersônico sob ambientes térmicos. *Métodos Computacionais em Mecânica Aplicada e Engenharia*, v. 325, 2017, p. 416-433. ISSN0045-7825. Disponível em: <https://doi.org/10.1016/j.cma.2017.07.014> . Acesso em: 29/08/2023.
- [22] ZHANG, LW; CANÇÃO, ZG; LIEW, KM Computação de propriedades aerotermoelásticas e controle ativo de flutter de painéis compósitos funcionalmente graduados reforçados com CNT em fluxo de ar supersônico. *Métodos Computacionais em Mecânica Aplicada e Engenharia*, v. 300, 2016, p. 427-441. ISSN0045-7825. Disponível em: <https://doi.org/10.1016/j.cma.2015.11.029> . Acesso em: 29/08/2023.
- [23] LEE, HP Flutter de uma haste cantilever com uma massa concentrada relocável. *Métodos Computacionais em Mecânica Aplicada e Engenharia*, v. 144, n. 1-2, 1997, pág. 23-31. ISSN0045-7825. Disponível em: [https://doi.org/10.1016/S0045-7825\(96\)01056-0](https://doi.org/10.1016/S0045-7825(96)01056-0) . Acesso em: 29/08/2023.
- [24] YONGNIAN, Yang. Um método de simulação digital para análise de vibração. *Métodos Computacionais em Mecânica Aplicada e Engenharia*, v. 56, n. 3, 1986, pág. 329-337. ISSN0045-7825. Disponível em: [https://doi.org/10.1016/0045-7825\(86\)90045-9](https://doi.org/10.1016/0045-7825(86)90045-9) . Acesso em: 29/08/2023.
- [25] STAROSSEK, U.; FERENCZI, T.; PRIEBE, J. Estabilizador de vibração de asa excêntrica para pontes – Análise, testes, projeto e custos. *Estruturas de Engenharia*, v. 172, 2018, p. 1073-1080. ISSN0141-0296. Disponível em: <https://doi.org/10.1016/j.engstruct.2018.06.056> . Acesso em: 29/08/2023.
- [26] BERA, Kamal Krishna; BANERJEE, Arnab. Uma matriz de rigidez dinâmica consistente para análise de vibração de tabuleiros de pontes. *Computadores e Estruturas*, v. 286, 2023, p. 107107. ISSN0045-7949. Disponível em: <https://doi.org/10.1016/j.compstruc.2023.107107> . Acesso em: 29/08/2023.

- [27] WU, Bo et al. Investigação de características não lineares e transicionais de flutter variando com os ângulos de ataque do vento para algumas seções típicas com diferentes razões laterais. *Revista de Fluidos e Estruturas*, v. 121, 2023, p. 103934. ISSN0889-9746. Disponível em: <https://doi.org/10.1016/j.jfluidstructs.2023.103934> . Acesso em: 29/08/2023.
- [28] CHAJJED, Sandip et al. Predição probabilística de flutter de coalescência usando medidas: Aplicação ao método de margem de flutter. *Jornal de Som e Vibração*, v. 117819, 2023. ISSN 0022-460X. Disponível em: <https://doi.org/10.1016/j.jsv.2023.117819> . Acesso em: 29/08/2023.
- [29] ZHANG, Hang et al. Supressão de vibração de um aerofólio usando um dissipador de energia não linear combinado com um coletor de energia piezoelétrico. *Comunicações em Ciência Não Linear e Simulação Numérica*, v. 125, 2023, p. 107350. ISSN 1007-5704. Disponível em: <https://doi.org/10.1016/j.cnsns.2023.107350> . Acesso em: 29/08/2023.
- [30] WANG, Jiayi et al. Flutter aeroelástico de feixes de nanocompósitos controlados ativamente com uma trinca de borda aberta. *Ciência e Tecnologia Aeroespacial*, v. 141, 2023, p. 108498. ISSN 1270-9638. Disponível em: <https://doi.org/10.1016/j.ast.2023.108498> . Acesso em: 29/08/2023.
- [31] TSUSHIMA, Natsuki; SAITOH, Kenichi; NAKAKITA, Kazuyuki. Características estruturais e aeroelásticas do modelo de asa para teste de flutter transônico em túnel de vento fabricado por manufatura aditiva com ligas AlSi10Mg. *Ciência e Tecnologia Aeroespacial*, v. 140, 2023, p. 108476. ISSN 1270-9638. Disponível em: <https://doi.org/10.1016/j.ast.2023.108476> . Acesso em: 29/08/2023.
- [32] PALAKURTHY, Seshendra et al. Estudo numérico do efeito de microvórtices na vibração caótica. *Revista de Matemática Computacional e Aplicada*, v. 436, 2024, p. 115401. ISSN0377-0427. Disponível em: <https://doi.org/10.1016/j.cam.2023.115401> . Acesso em: 29/08/2023.
- [33] DUAN, Xianbo et al. Mecanismo de influência e avaliação quantitativa dos principais fatores que afetam a estabilidade de vibração de um ventilador transônico. *Ciência e Tecnologia Aeroespacial*, v. 138, 2023, p. 108312. ISSN 1270-9638. Disponível em: <https://doi.org/10.1016/j.ast.2023.108312> . Acesso em: 29/08/2023.
- [34] KURIAKOSE, Vinu M.; SREEHARI, VM Análise de vibração e flutter de placas compostas danificadas sob ambiente térmico e seu controle passivo usando patches piezoelétricos. *Compósitos Parte C: Acesso Aberto*, v. 11, 2023, p. 100361. ISSN 2666-6820. Disponível em: <https://doi.org/10.1016/j.jcomc.2023.100361> . Acesso em: 29/08/2023.
- [35] GOYANIUK, L. et al. O potencial de extração de energia da vibração acoplada ao pitch-heave. *Jornal de Som e Vibração*, v. 555, 2023, p. 117714. ISSN0022-460X. Disponível em: <https://doi.org/10.1016/j.jsv.2023.117714> . Acesso em: 29/08/2023.